3602 *Inorg. Chem.* **2010**, *49*, 3602–3609
DOI: 10.1021/ic901869t

Inorganic Chemistry
Forum Article

Dioxygen Activation for the Self-Degradation of Heme: Reaction Mechanism and Regulation of Heme Oxygenase

Toshitaka Matsui,* Mari Iwasaki, Ryota Sugiyama, Masaki Unno,† and Masao Ikeda-Saito*

Institute of Multidisciplinary Research for Advanced Materials, Tohoku University, Katahira, Aoba, Sendai 980-8577, Japan. †Present address: Frontier Research Center for Applied Atomic Sciences, Ibaraki University, Naka, Ibaraki 319-1106, Japan.

Received September 22, 2009

Heme oxygenase (HO) catalyzes the regiospecific conversion of heme to biliverdin, CO, and free iron through three successive oxygenation reactions. HO catalysis is unique in that all three O_2 activations are performed by the substrate itself. This Forum Article overviews our current understanding on the structural and biochemical properties of HO catalysis, especially its first and third oxygenation steps. The HO first step, regiospecific hydroxylation of the porphyrin α-*meso*-carbon atom, is of particular interest because of its sharp contrast to O_2 activation by cytochrome P450. HO was proposed to utilize the FeOOH species but not conventional ferryl hemes as a reactive intermediate for self-hydroxylation. We have succeeded in preparing and characterizing the FeOOH species of HO at low temperature, and our analyses of its reaction, together with mutational and crystallographic studies, reveal that protonation of FeOOH by a distal water molecule is critical in promoting the unique self-hydroxylation. The second oxygenation is a rapid, spontaneous autooxidation of the reactive α-*meso*-hydroxyheme in which the HO enzyme does *not* play a critical role. Further O_2 activation by verdoheme cleaves its porphyrin macrocycle to form biliverdin and free ferrous iron. This third step has been considered to be a major rate-determining step of HO catalysis to regulate the enzyme activity. Our reaction analysis strongly supports the FeOOH verdoheme as the key intermediate of the ring-opening reaction. This mechanism is very similar to that of the first *meso*-hydroxylation, and the distal water is suggested to enhance the third step as expected from the similarity. The HO mechanistic studies highlight the catalytic importance of the distal hydrogen-bonding network, and this manuscript also involves our attempts to develop HO inhibitors targeting the unique distal structure.

Introduction

O_2 activation by heme enzymes including peroxidase, catalase, and cytochrome P450 has been extensively studied over the last 4 decades. As a common reactive species, these enzymes normally employ compound I, a ferryl ($O{=}Fe^{IV}$) heme paired with a porphyrin cation radical. Biochemical studies on these heme enzymes thus have focused on the formation process of compound I and its reactivity.[1−3] Poulos and Kraut proposed a so-called "push−pull" mechanism for explaining the extremely high reactivity of peroxidase with H_2O_2 to afford compound I.[4] In this mechanism, the distal histidine first serves as a general base to facilitate the H_2O_2 binding to the heme iron. The protonated distal histidine then transfers a proton to the distal oxygen atom of the iron hydroperoxy (FeOOH) species. Polarization of the O−O bond is enhanced by this protonation as well as by a positively charged arginine residue to promote its heterolytic cleavage, leading to the facile formation of compound I ("pull" effect). Proximal histidine of peroxidase has a deprotonated histidinate character, and the "push" effect of this anionic character of the axial heme ligand contributes to the charge separation as well. O_2 activation by hemes in catalase and cytochrome P450 can also be interpreted in line with the "push−pull" mechanism.

Heme also activates molecular oxygen for its own biological degradation. The heme catabolism is initiated by a group of enzymes termed heme oxygenases (HOs). HO catalyzes the regiospecific conversion of heme to biliverdin IXα, CO, and free iron through three successive steps of O_2 activation involving the uptake of a total of seven electrons (Figure 1).[5−7] HO catalysis is unique in that all of the O_2

*To whom correspondence should be addressed. E-mail: matsui@tagen.tohoku.ac.jp (T.M.), mis2@tagen.tohoku.ac.jp (M.I.-S.). Telephone: +81-22-217-5116. Fax: +81-22-217-5118.

(1) Dunford, H. B.; Stillman, J. S. *Coord. Chem. Rev.* **1987**, *19*, 187–251.
(2) Schonbaum, G. R.; Chance, B. In *The Enzymes*, 3rd ed.; Boyer, P. D., Ed.; Academic Press: New York, 1976; Vol. *13*, pp 363−408.
(3) Dawson, J. H.; Holm, R. H.; Trudell, J. R.; Barth, G.; Linder, R. E.; Bunnenberg, E.; Djerassi, C.; Tang, S. C. *J. Am. Chem. Soc.* **1976**, *98*, 3707–3709.
(4) Poulos, T. L.; Kraut, J. *J. Biol. Chem.* **1980**, *255*, 8199–8205.
(5) Tenhunen, R.; Marver, H. S.; Schmid, R. *J. Biol. Chem.* **1969**, *244*, 6388–6394.
(6) Yoshida, T.; Kikuchi, G. *J. Biol. Chem.* **1978**, *253*, 4230–4236.
(7) Ortiz de Montellano, P. R. *Acc. Chem. Res.* **1998**, *31*, 543–549.

Published on Web 04/12/2010

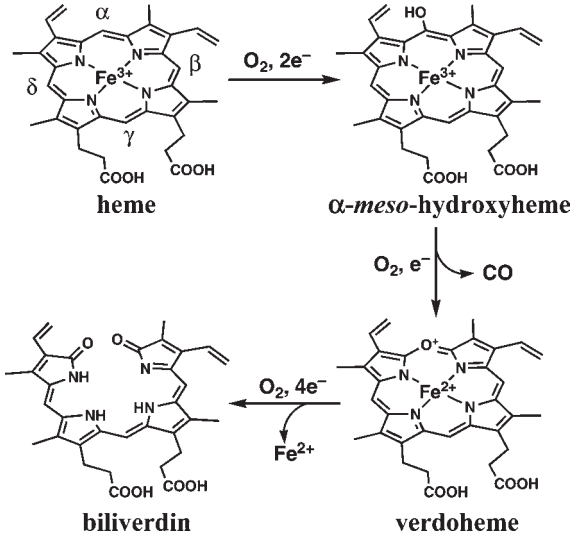

Figure 1. Heme degradation sequence catalyzed by HO.

activations are performed by the substrate itself, as evidenced by the absence of any other cofactor in HO.[6,7] The conventional heme enzymes, such as peroxidase, catalase, and cytochrome P450, strictly avoid such self-oxidation of the prosthetic group, which would result in enzyme inactivation. Thus, the HO enzyme must have a protein architecture that enables the unique O_2 activation for heme self-degradation. HO was first identified in mammals as two isoforms, an inducible HO-1 and a constitutive HO-2.[8] In mammals, electrons required for catalytic turnover are provided by NADPH−cytochrome P450 reductase,[9] and biliverdin is rapidly reduced by biliverdin reductase to bilirubin. In addition to the HO's well-established capacity in mammalian heme catabolism, new results have accumulated on the HO's extended roles in iron homeostasis, antioxidant defense, cellular signaling, and O_2 sensing.[6,10−13] HO is also found in plants (producing light-harvesting pigments) and some pathogenic bacteria, where it acquires iron from the host heme.[14−18] In this Forum Article, we review our current understanding on the structural and biochemical properties of HO catalysis. Our study proposes critical functioning of the FeOOH species in HO heme self-oxidation and highlights the catalytic importance of the distal hydrogen-bonding network in its unique O_2 activation. This Forum Article also includes the results of our attempts to develop HO-specific inhibitors targeting the critical distal hydrogen-bonding network.

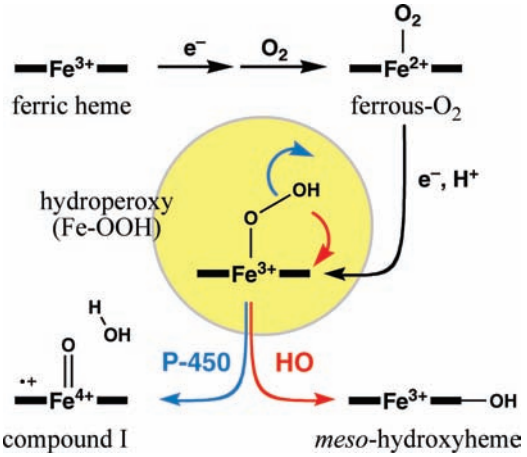

Figure 2. Comparison of O_2 activation by HO and cytochrome P450.

Overview of Three Oxygenations in HO Catalysis

HO catalysis consists of three self-mono-oxygenation reactions (Figure 1). In the first step, heme activates one molecule of O_2 for the regiospecific self-hydroxylation of the porphyrin α-*meso*-carbon atom. The resulting α-*meso*-hydroxyheme reacts in the second step with another O_2 to yield verdoheme and CO. The third O_2 activation by verdoheme cleaves the porphyrin macrocycle to afford biliverdin and free ferrous iron. In these three oxygenations, the HO enzyme is involved to a much lesser extent in the second step in comparison with the other two steps. The second step is a spontaneous autooxidation of the reactive α-*meso*-hydroxyheme and has been reported to proceed rapidly even in the absence of the enzyme.[19] This Forum Article thus focuses on the first and third steps of the HO reactions.

The first O_2 activation by HO, *meso*-hydroxylation, is in distinct contrast with that by cytochrome P450 (Figure 2). While both cytochrome P450 and HO activate molecular oxygen by utilizing two electrons at their heme centers, the former monooxygenates exogenous substrates and the latter hydroxylates the heme itself. The HO first step utilizes reaction intermediates similar to those found in cytochrome P450 and peroxidase catalysis (Figure 2), and the HO mechanistic studies have benefited from the enormous data accumulated on these classical heme enzymes. Consequently, the first O_2 activation in HO catalysis has been successfully clarified in detail.[20,21] To the contrary, verdoheme ring opening in the HO third step has remained unclear because the reaction profiles and spectroscopic properties of the verdoheme intermediates were not understood well. We have recently been successful in untangling the mechanistic outline and kinetic properties of the HO third step.[22,23] In the following sections, reaction mechanisms of the HO first and third steps are discussed in relation to the enzyme structures.

(8) Maines, M. D.; Trakshel, G. M.; Kutty, R. K. *J. Biol. Chem.* **1986**, *261*, 411–419.
(9) Schacter, B. A.; Nelson, E. B.; Marver, H. S.; Masters, B. S. S. *J. Biol. Chem.* **1972**, *247*, 3601–3607.
(10) Maines, M. D. *Annu. Rev. Pharmacol. Toxicol.* **1997**, *37*, 517–554.
(11) Poss, K. D.; Tonegawa, S. *Proc. Natl. Acad. Sci. U.S.A.* **1997**, *94*, 10925–10930.
(12) Suematsu, M.; Ishimura, Y. *Hepatology* **2000**, *31*, 3–6.
(13) Williams, S. E.; Wootton, P.; Mason, H. S.; Bould, J.; Iles, D. E.; Riccardi, D.; Peers, C.; Kemp, P. J. *Science* **2004**, *306*, 2093–2097.
(14) Cornejo, J.; Willows, R. D.; Beale, S. I. *Plant J.* **1998**, *15*, 99–107.
(15) Davis, S. J.; Kurepa, J.; Vierstra, R. D. *Proc. Natl. Acad. Sci. U.S.A.* **1999**, *96*, 6541–6546.
(16) Schmitt, M. P. *J. Bacteriol.* **1997**, *179*, 838–845.
(17) Wandersman, C.; Stojiljkovic, I. *Curr. Opin. Microbiol.* **2000**, *3*, 215–220.
(18) Genco, C. A.; Dixon, D. W. *Mol. Microbiol.* **2001**, *39*, 1–11.
(19) Morishima, I.; Fujii, H.; Shiro, Y.; Sano, S. *Inorg. Chem.* **1995**, *34*, 1528–1535.
(20) Colas, C.; Ortiz de Montellano, P. R. *Chem. Rev.* **2003**, *103*, 2305–2332.
(21) Unno, M.; Matsui, T.; Ikeda-Saito, M. *Nat. Prod. Rep.* **2007**, *24*, 553–570.
(22) Matsui, T.; Nakajima, A.; Fujii, H.; Mansfield Matera, K.; Migita, C. T.; Yoshida, T.; Ikeda-Saito, M. *J. Biol. Chem.* **2005**, *280*, 36833–36840.
(23) Matsui, T.; Omori, K.; Jin, H.; Ikeda-Saito, M. *J. Am. Chem. Soc.* **2008**, *130*, 4220–4221.

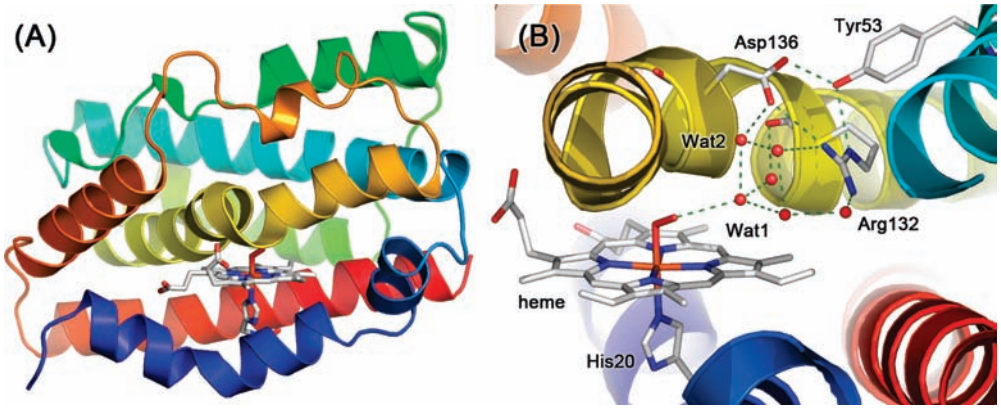

Figure 3. Crystal structure of the ferrous-O_2 heme-HmuO complex:[25] (A) overall structure; (B) heme environment (PDB code 1 V8X). Red balls represent oxygen atoms of the water molecules.

First *meso*-Hydroxylation of Heme

The initial O_2 activation of HO shares similar features with that of cytochrome P450. In both HO and cytochrome P450, an initial step for the O_2 activation is the reduction of the ferric heme iron to the ferrous state, which binds O_2 (Figure 2). Subsequent one-electron reduction and protonation of the ferrous-O_2 heme give a ferric hydroperoxy species (FeOOH). In cytochrome P450 as well as peroxidase and catalase, the terminal oxygen of FeOOH is thought to be liberated as water to give compound I or its equivalent as an active species. A strong electron "push" by an axial thiolate ligand is believed to promote heterolysis in cytochrome P450. The crystal structures of HO [24−27] show that the heme pocket is not designed for enhancing the O−O bond heterolysis (Figure 3 for HmuO, HO from *Corynebacterium diphtheriae*).[26] The heme group in HO is tightly sandwiched between two helices termed the "proximal" and "distal" helices (Figure 3A, blue and yellow, respectively). The proximal helix contains an axial His ligand, which is essentially neutral as those in myoglobin and hemoglobin.[28] The distal helix of HO is kinked above the heme plane around the two conserved Gly residues and is in close contact with the heme group to sterically restrict access to all of the meso positions except for the α-*meso*-carbon. This distal structure gives a rationale for the α-*meso*-selectivity in the HO first step. There is no general acid−base catalyst like the distal histidine in peroxidases, and polar residues are located too far away to interact directly with the heme-bound O_2 species (Figure 3). Neither a strong "push" nor "pull" effect is expected for the HO active site. In fact, HO compound I generated artificially is directly shown not to be responsible for the heme hydroxylation.[29]

The reactive intermediate of the HO first step has been proposed to be the FeOOH species. As a surrogate of O_2 and two electrons, H_2O_2 efficiently supports the α-*meso*-hydroxyheme formation (Figure 2), whereas most alkyl and acyl hydroperoxides afford the inactive ferryl hemes.[30] A small peroxide, ethyl hydroperoxide, was reported to produce α-*meso*-ethoxyheme in a relatively lower yield, suggesting an intramolecular ethoxy transfer by an FeOOEt intermediate.[31] The FeOOH species of HO has been successfully observed at cryogenic temperatures, and its conversion to α-*meso*-hydroxyheme without detectable intermediates is indicative of self-hydroxylation by FeOOH.[32] The HO enzyme is likely to endow FeOOH with a special reactivity to transfer its terminal OH group into the α-*meso*-carbon because most heme enzymes cleave the O−O bond to form ferryl hemes without OH transfer.

The ferrous-O_2 complex is an immediate precursor of the FeOOH species (Figure 2) and could serve as a reasonable structural model of the highly reactive FeOOH intermediate. We have successfully determined the crystal structure of the ferrous-O_2 complex of HmuO (Figure 3).[26] The steric constraints imposed by the distal helix direct the terminal oxygen atom of the ferrous-O_2 complex toward the heme α-*meso*-carbon. The Fe−O−O angle in oxy-HO is unusually acute (~110°), as was originally deduced from the resonance Raman analysis.[26,33] This acute angle allows the terminal oxygen to come within van der Waals contact with the α-*meso*-carbon and may help explain the unique OH transfer. Another salient feature of the O_2 moiety is its interaction with an extended hydrogen-bonding network of the HO distal side. The terminal oxygen atom of the heme-bound O_2 interacts also with a water molecule (Wat1 in Figure 3B), which is a part of the hydrogen-bonding network containing a water cluster and a catalytically critical distal Asp residue (Asp136 in HmuO, Figure 3B).

The distal Asp, which is conserved in most mammalian, plant, and bacterial HOs, interacts with the heme ligand through intervening water molecules (Wat1 and Wat2 in Figure 3B).[24,25,34] The mutagenesis studies on mammalian

(24) Schuller, D. J.; Wilks, A.; Ortiz de Montellano, P. R.; Poulos, T. L. *Nat. Struct. Biol.* **1999**, *6*, 860–867.
(25) Sugishima, M.; Omata, Y.; Kakuta, Y.; Sakamoto, H.; Noguchi, M.; Fukuyama, K. *FEBS Lett.* **2000**, *471*, 61–66.
(26) Unno, M.; Matsui, T.; Chu, G. C.; Couture, M.; Yoshida, T.; Rousseau, D. L.; Olson, J. S.; Ikeda-Saito, M. *J. Biol. Chem.* **2004**, *279*, 21055–21061.
(27) Bianchetti, C. M.; Yi, L.; Ragsdale, S. W.; Phillips, G. N., Jr. *J. Biol. Chem.* **2007**, *282*, 37624–37631.
(28) Takahashi, S.; Wang, J.; Rousseau, D. L.; Ishikawa, K.; Yoshida, T.; Host, J. R.; Ikeda-Saito, M. *J. Biol. Chem.* **1994**, *269*, 1010–1014.
(29) Matsui, T.; Kim, S. H.; Jin, H.; Hoffman, B. M.; Ikeda-Saito, M. *J. Am. Chem. Soc.* **2006**, *128*, 1090–1091.
(30) Wilks, A.; Ortiz de Montellano, P. R. *J. Biol. Chem.* **1993**, *268*, 22357–22362.
(31) Wilks, A.; Torpey, J.; Ortiz de Montellano, P. R. *J. Biol. Chem.* **1994**, *269*, 29553–29556.
(32) Davydov, R. M.; Yoshida, T.; Ikeda-Saito, M.; Hoffman, B. M. *J. Am. Chem. Soc.* **1999**, *121*, 10656–10657.
(33) Takahashi, S.; Ishikawa, K.; Takeuchi, N.; Ikeda-Saito, M.; Yoshida, T.; Rousseau, D. L. *J. Am. Chem. Soc.* **1995**, *117*, 6002–6006.
(34) Hirotsu, S.; Chu, G. C.; Unno, M.; Lee, D. S.; Yoshida, T.; Park, S. Y.; Shiro, Y.; Ikeda-Saito, M. *J. Biol. Chem.* **2003**, *279*, 11937–11947.

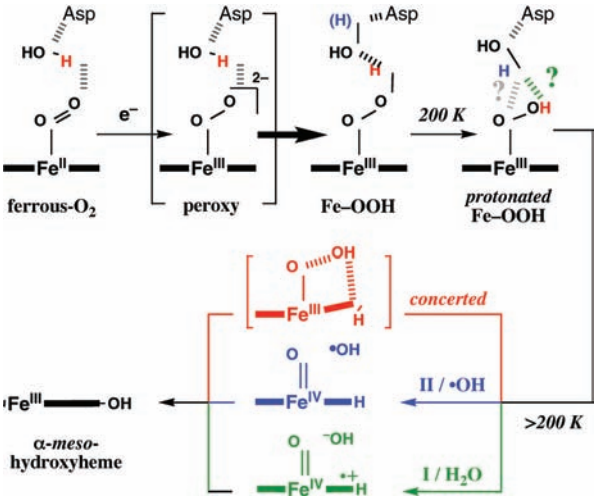

Figure 4. Mechanisms proposed for O_2 activation in the HO first step with three possible pathways of the OH transfer: (red) a concerted self-hydroxylation; (blue) a recombination of compound II with hydroxyl radical generated transiently; (green) a hydroxide addition to compound I.

HO-1 have led to a proposal that the carboxylate moiety of the distal Asp is indispensable for *meso*-hydroxylation.[35,36] The distal Asp was suggested to function as a hydrogen-bond *acceptor* to prevent protonation of FeOOH by Wat1, thus stabilizing the FeOOH intermediate.[37] This proposal, however, contradicts the observed absence of carboxyl residues in the distal pocket of some bacterial HOs.[38,39] Our comprehensive study on the HmuO distal Asp variants concludes that the distal Asp itself is not directly involved in the O_2 activation but stabilizes the water network to place the catalytically critical Wat1 at a position suitable for efficient FeOOH activation.[40] Moreover, we have shown that the proton *donation* is critical for *meso*-hydroxylation as discussed below.

A cryoreduction method has been successfully applied for the direct observation of the highly reactive FeOOH species. The ferrous-O_2 heme of HO-1 is reduced by γ- or β-ray irradiation at liquid nitrogen or helium temperatures (Figure 4).[32,41,42] The putative peroxy form ($FeOO^-$) is immediately protonated to afford FeOOH even near 4 K, where no heavy atom movement is expected to take place (Figure 4).[43] The efficient proton donor in HO is the Wat1 molecule, which forms a hydrogen-bonding interaction with the distal oxygen atom of the ferrous-O_2 heme (Figure 3B). The Asp140 to Ala replacement substantially suppresses proton transfer to accumulate the $FeOO^-$ species, consistent with displacement and/or fluctuation of the Wat1 molecule.[44] Annealing of wild-type FeOOH to 200 K results in further protonation of the dioxygen center (Figure 4).[44] The donor of this second proton is again most likely to be Wat1, because FeOOH in the D140A variant lacks the second proton. The *protonated* FeOOH in the wild type (Figure 4) directly converts to iron(III) hydroxyheme above 200 K with a significant solvent isotope effect (k_H/k_D = 2.3 at 215 K), indicating critical functioning of the second proton in the FeOOH activation. The *nonprotonated* FeOOH in the D140A mutant does not afford the hydroxyheme product.[45] These observations together with a secondary isotope effect observed upon deuteration of the meso protons[45] suggest a concerted *meso*-hydroxylation process: proton transfer to FeOOH through Wat1 occurring in synchrony with bond formation between the terminal oxygen and the α-*meso*-carbon (Figure 4, red). A second protonation by Wat1 is expected to take place at the terminal oxygen of the FeOOH species (Figure 4) and to facilitate the compound I formation by the "*pull*" effect. The direct contact of the terminal oxygen and α-*meso*-carbon may be indispensable for self-hydroxylation. Alternatively, the second protonation might occur at the proximal oxygen of FeOOH. Crystallographic analysis on the reactive FeOOH intermediate is underway to address the protonation site.

Theoretical studies have proposed mechanisms other than the concerted hydroxylation (Figure 4, blue and green).[46,47] The transition state of the concerted reaction is found to be highly strained, and a large activation energy has been estimated. The calculations favor stepwise mechanisms including an initial O−O bond cleavage, followed by the rebinding of a liberated OH group to the α-*meso*-carbon. The O−O bond heterolysis, followed by the addition of an OH anion[46] (Figure 4, green), is ruled out because compound I cannot afford *meso*-hydroxyheme.[29,47] Alternatively, the O−O bond might be cleaved homolytically to produce compound II and hydroxyl radical (•OH; Figure 4, blue). Although compound II alone is inactive for self-hydroxylation,[30] the reactivity of the hydroxyl radical transiently generated above the *meso*-carbon is yet to be experimentally evaluated. A recent QM/MM study concludes a very small activation energy for the radical addition, thereby making the reaction a nonsynchronous but *effectively concerted* pathway.[48] In this scheme, the distal water cluster holds the highly reactive hydroxyl radical in an orientation for the rapid and exclusive attack on the α-*meso*-carbon.[48]

Third Redox-Dependent Ring Opening of Verdoheme

The *meso*-hydroxyheme produced in the HO first step is converted into iron(II) verdoheme in the second step (Figure 1). Then, at the third stage of heme degradation, the macrocycle of iron(II) verdoheme is cleaved to afford

(35) Fujii, H.; Zhang, X.; Tomita, T.; Ikeda-Saito, M.; Yoshida, T. *J. Am. Chem. Soc.* **2001**, *123*, 6475–6484.
(36) Lightning, L. K.; Huang, H.; Moenne-Loccoz, P.; Loehr, T. M.; Schuller, D. J.; Poulos, T. L.; Ortiz de Montellano, P. R. *J. Biol. Chem.* **2001**, *276*, 10612–10619.
(37) Lad, L.; Wang, J.; Li, H.; Friedman, J.; Bhaskar, B.; Ortiz de Montellano, P. R.; Poulos, T. L. *J. Mol. Biol.* **2003**, *330*, 527–538.
(38) Schuller, D. J.; Zhu, W.; Stojiljkovic, I.; Wilks, A.; Poulos, T. L. *Biochemistry* **2001**, *40*, 11552–11558.
(39) Friedman, J.; Lad, L.; Li, H.; Wilks, A.; Poulos, T. L. *Biochemistry* **2004**, *43*, 5239–5245.
(40) Matsui, T.; Furukawa, M.; Unno, M.; Tomita, T.; Ikeda-Saito, M. *J. Biol. Chem.* **2005**, *280*, 2981–2989.
(41) Denisov, I. G.; Ikeda-Saito, M.; Yoshida, T.; Sligar, S. G. *FEBS Lett.* **2002**, *532*, 203–206.
(42) Garcia-Serres, R.; Davydov, R. M.; Matsui, T.; Ikeda-Saito, M.; Hoffman, B. M.; Huynh, B. H. *J. Am. Chem. Soc.* **2007**, *129*, 1402–1412.
(43) Davydov, R.; Chemerisov, S.; Werst, D. E.; Rajh, T.; Matsui, T.; Ikeda-Saito, M.; Hoffman, B. M. *J. Am. Chem. Soc.* **2004**, *126*, 15960–15961.
(44) Davydov, R.; Kofman, V.; Fujii, H.; Yoshida, T.; Ikeda-Saito, M.; Hoffman, B. M. *J. Am. Chem. Soc.* **2002**, *124*, 1798–1808.
(45) Davydov, R.; Matsui, T.; Fujii, H.; Ikeda-Saito, M.; Hoffman, B. M. *J. Am. Chem. Soc.* **2003**, *125*, 16208–16209.
(46) Kumar, D.; de Visser, S. P.; Shaik, S. *J. Am. Chem. Soc.* **2005**, *127*, 8204–8213.
(47) Kamachi, T.; Yoshizawa, K. *J. Am. Chem. Soc.* **2005**, *127*, 10686–10692.
(48) Chen, H.; Moreau, Y.; Derat, E.; Shaik, S. *J. Am. Chem. Soc.* **2008**, *130*, 1953–1965.

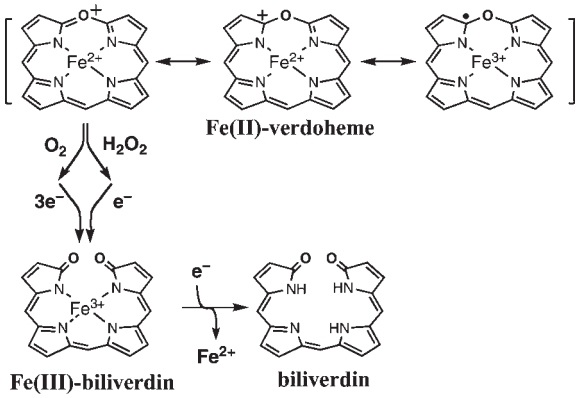

Figure 5. Dual pathway of verdoheme ring opening supported by O_2 and H_2O_2.

biliverdin and the free ferrous ion with the consumption of one O_2 molecule and four reducing equivalents (Figure 1). This HO third step is considered to be the major rate-determining step to regulate the enzyme activity *in vivo*.[49] Nevertheless, its mechanism has been the least understood among three oxygenation steps in HO catalysis.

Nonenzymatic conversion of verdoheme to biliverdin can take place through hydrolysis or redox reactions using O_2 or H_2O_2.[50−52] The HO enzyme incorporates an oxygen atom of O_2 rather than of water into biliverdin.[53] The verdoheme−HO complex was originally reported not to react with H_2O_2 and to utilize exclusively O_2 for biliverdin formation.[7,30] This observation suggested that this HO third step was mechanistically distinct from the HO first step, which can proceed also through the H_2O_2-shunt pathway.[30] The lack of reactivity with H_2O_2, however, occurs only in the case of iron(III) verdoheme. We have demonstrated that the iron(II) verdoheme−HO-1 complex readily reacts with H_2O_2 to afford biliverdin under reducing conditions (Figure 5).[22] The dual pathway degradation of verdoheme is initiated by the binding of either O_2 or H_2O_2 on iron(II) verdoheme to allow the direct observation of ring-opening intermediates. While the nature of these intermediates is yet to be determined, the reduction of these intermediates results in iron(III) biliverdin. Further one-electron reduction releases the ferrous iron to afford biliverdin. O_2 may bind either on the verdoheme iron or on a radical generated at the α-pyrrole carbon because of the possible resonance of iron(II) verdoheme involving changes in the redox state of iron (Figure 5). This is also the case for H_2O_2, which can bind on either the iron or the α-pyrrole cation. Even in the chemical model reactions, the initial binding sites of O_2 and H_2O_2 have never been identified.

The H_2O_2 pathway is less complicated than the O_2 pathway because of the smaller number of reduction steps to afford biliverdin (Figure 5). In the H_2O_2 reaction, the peroxide binding would produce the FeOOH or ring−OOH verdoheme complexes that may be deprotonated to form a

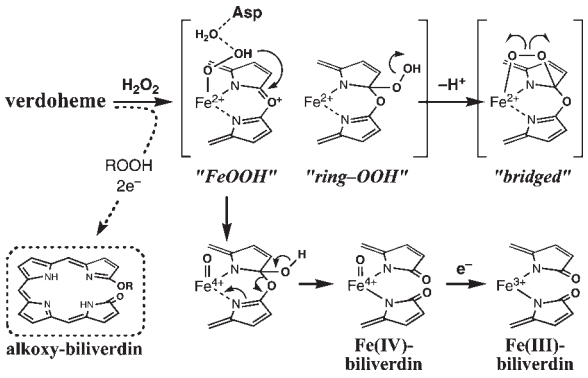

Figure 6. Proposed mechanism for the ring opening of verdoheme.

bridged intermediate (Figure 6). All three possible intermediates could generate biliverdin upon O−O bond cleavage. To gain insight into the mode of the reaction, we have examined the verdoheme ring-opening reactions supported by small alkyl hydroperoxides (ROOH) like CH_3OOH.[23] The FeOOR pathway could add the alkoxy moiety to one end of biliverdin, while the ring−OOR pathway would give normal biliverdin. When the ring opening involves the bridged intermediate, no linear tetrapyrrole should be observed because the alkyl group is hardly liberated. Product analysis of the CH_3OOH reaction finds exclusive formation of methoxybiliverdin (Figure 6), indicating the FeOOR species as the key intermediate. Therefore, in the H_2O_2 pathway, the corresponding FeOOH verdoheme is likely to transfer its terminal OH group into the α-pyrrole carbon (Figure 6). Deprotonation of the OH adduct and the following reduction could afford iron(III) biliverdin and then ferrous iron and biliverdin.

The OH transfer to the porphyrin ring by FeOOH is very similar to that of the HO first step, *meso*-hydroxylation of heme (Figure 4). This mechanistic similarity is rational for catalyzing multiple-step reactions by a single enzyme: HO utilizes the common protein architecture to promote both the first and third O_2 activations. Product yields in the H_2O_2-supported verdoheme degradation are lowered by the distal Asp substitutions in HO-1 as observed for the first step.[22,35,36,40] Very similar reductions in the product yield are observed for the O_2-dependent verdoheme degradation, and the effects of the distal Asp substitutions are essentially the same for the O_2 and H_2O_2 pathways. These observations strongly support the water-mediated activation of the FeOOH verdoheme in both the O_2- and H_2O_2-dependent ring openings (Figure 6).

Contrary to our mechanistic proposal, a crystal structure reported for the iron(II) verdoheme−human HO-1 complex showed no water in the distal heme pocket.[54] The verdoheme iron in the crystal was five-coordinate without an exogenous ligand; however, spectroscopic studies unambiguously indicate that the iron(II) verdoheme is six-coordinate low-spin, possibly with a water (hydroxide) ligand.[55,56] Another crystallographic study reported recently found water molecules in

(49) Liu, Y.; Ortiz de Montellano, P. R. *J. Biol. Chem.* **2000**, *275*, 5297–5307.
(50) Fuhrhop, J. H.; Kruger, P. *Liebigs Ann. Chem.* **1977**, 360–370.
(51) Saito, S.; Itano, H. A. *Proc. Natl. Acad. Sci. U.S.A.* **1982**, *79*, 1393–1397.
(52) Sano, S.; Sano, T.; Morishima, I.; Shiro, Y.; Maeda, Y. *Proc. Natl. Acad. Sci. U.S.A.* **1986**, *83*, 531–535.
(53) Docherty, J. C.; Schacter, B. A.; Firneisz, G. D.; Brown, S. B. *J. Biol. Chem.* **1984**, *259*, 13066–13069.
(54) Lad, L.; Ortiz de Montellano, P. R.; Poulos, T. L. *J. Inorg. Biochem.* **2004**, *98*, 1686–1695.
(55) Takahashi, S.; Mansfield Matera, K.; Fujii, H.; Zhou, H.; Ishikawa, K.; Yoshida, T.; Ikeda-Saito, M.; Rousseau, D. L. *Biochemistry* **1997**, *36*, 1402–1410.
(56) Damaso, C. O.; Bunce, R. A.; Barybin, M. V.; Wilks, A.; Rivera, M. *J. Am. Chem. Soc.* **2005**, *127*, 17582–17583.

the rat verdoheme−HO-1 distal pocket.[57] However, the absorption spectrum of the rat HO-1 crystal was apparently different from that of the iron(II) verdoheme−HO complex. The rat HO-1 crystal might contain an iron(II) verdoheme neutral radical as the authors stated, which is a one-electron-reduced form of the so-called iron(II) verdoheme and is never generated during HO catalysis. This new structure thus does not prove the presence of the distal water cluster and the aquo ligand in the catalytically relevant iron(II) verdoheme complex.[57] In order to reassess the verdoheme structure, we have recently crystallized the iron(II) verdoheme−HmuO complex.[58] In our structure refined to 2.0 Å resolution, a spherical electron density corresponding to the aqua ligand and water molecules is clearly observed at the verdoheme distal side, consistent with our proposed water-assisted O_2 activation mechanism.[22,23] Absorption spectra of our HmuO crystals indicate no significant changes on the verdoheme center upon crystallization and X-ray irradiation. Further structural refinement and spectroscopic assessment on the verdoheme status will provide a definitive conclusion on the structure and O_2 activation mechanism of the fragile verdoheme intermediate.

Modulation of HO Catalysis by Ligands Targeting the Critical Distal Pocket Structure

Our structural and mechanistic studies have highlighted the catalytic importance of the HO distal pocket, which forms the well-extended hydrogen-bonding network and contains the critical water cluster (Figure 3). The unique structure allows us to propose that the distal hydrogen-bonding network is a potential target of a novel specific inhibitor of the HO enzyme. Small molecules may tightly bind to the distal pocket to interfere with HO catalysis. While metal-substituted hemes including tin and zinc porphyrins have been used as conventional HO inhibitors,[59] they are known to affect other proteins including soluble guanylate cyclase and NO synthase as well.[60−62] The metalloporphyrin inhibitors normally have low selectivity for the mammalian HO isoforms, HO-1 and HO-2. The distal pocket ligand as an alternative inhibitor of HO could compensate for the disadvantages of the metalloporphyrin inhibitors and may exhibit isoform selectivity by recognizing the subtle structural distinctions in the distal sites of the different isoforms. An isoform-selective inhibitor of HO that is an iron ligand having a tail interacting with the distal network has been reported.[63,64]

We have examined reactions of the heme−HO complexes with a variety of small molecules, namely, thiol compounds. The thiol group can be a ligand of the ferric heme iron, and its binding is easily monitored spectrophotometrically. Affinity of the thiols toward the ferric heme is normally low, and this

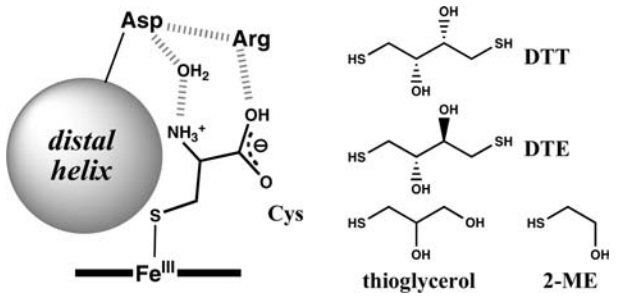

Figure 7. Possible interaction of heme-bound thiols in the HO active site.

Table 1. Equilibrium Dissociation Constants (K_d) of Thiol Compounds with Ferric Heme−HO Complexes [a]

	K_d/μM		
	human HO-1	human HO-2	HmuO
L-Cys	2330	2360	b
D-Cys	2310	673	b
L-Cys methyl ester	141	79	124
L-Cys ethyl ester	37	50	2,350
N-acetyl-L-Cys	*b*	*b*	*b*
glutathione	*b*	*b*	*b*
DL-dithiothreitol (DTT)	5.1 (4.7)[c]	34	244
dithioerythrothreitol (DTE)	4.6 (6.8)[c]	64	232
thioglycerol	61 (150)[c]	346	207
2-mercaptoethanol	208 (400)[c]	939	3,950

[a] K_d values were determined by spectral titration (404 nm) of the ferric heme−HO complexes (0.2−1 μM) with thiol compounds at 20 °C in a 0.1 M potassium phosphate buffer, pH 7.0. [b] Too high to determine (> 10 mM). [c] Values in parentheses are dissociation constants for rat HO-1.

suppresses nonspecific binding to the other heme enzymes. Moreover, bent ligation of the thiols, as with O_2, is expected to circumvent steric repulsion from the distal helix of HO (Figures 3 and 7). We have chosen a thiol-containing amino acid, Cys, as a starting compound whose amino and carboxyl groups are capable of hydrogen bonding and/or ionic interaction with surrounding polar residues and water molecules (Figure 7). L- and D-Cys bind as thiolates to the ferric heme−human HO complexes with moderate affinity. While Cys shows an affinity similar to that of the mammalian isoforms (human HO-1 and HO-2), the heme−HmuO complex hardly binds Cys (Table 1), indicating that even simple amino acids can discern subtle structural differences between the mammalian and bacterial HO. As listed in Table 1, modification of the amino group of L-Cys diminishes its binding ability for all of the HO enzymes possibly because of increased steric hindrance with the distal helix. In contrast, esterification of the carboxyl group drastically increases the affinity.

Further screening shows that DL-dithiothreitol (DTT) and its stereoisomer dithioerythrothreitol (DTE) bind to the mammalian HO with anomalously high affinity (Table 1). These compounds, especially DTE, show high HO-1 selectivity over HO-2 (6.7- and 14-fold for DTT and DTE, respectively). It should be noted that met myoglobin hardly binds DTT (K_d > 100 mM), even though its electronic and coordination structures of the ferric heme in met myoglobin are almost identical with those in HO.[28] Because thioglycerol lacking one of the thiol groups of DTT (Figure 7) shows 10-fold lower affinity than DTT, the noncoordinating thiol

(57) Sato, H.; Sugishima, M.; Sakamoto, H.; Higashimoto, Y.; Shimokawa, C.; Fukuyama, K.; Palmer, G.; Noguchi, M. *Biochem. J.* **2009**, *419*, 339–345.
(58) Matsui, T.; Unno, M.; Ikeda-Saito, M. Unpublished results.
(59) Maines, M. D. *Biochim. Biophys. Acta* **1981**, *673*, 339–350.
(60) Luo, D.; Vincent, S. R. *Eur. J. Pharmacol.* **1994**, *267*, 263–267.
(61) Grundemar, L.; Ny, L. *Trends Pharmacol. Sci.* **1997**, *18*, 193–195.
(62) Meffert, M. K.; Haley, J. E.; Schuman, E. M.; Schulman, H.; Madison, D. V. *Neuron* **1994**, *13*, 1225–1233.
(63) Vlahakis, J. Z.; Kinobe, R. T.; Bowers, R. J.; Brien, J. F.; Nakatsu, K.; Szarek, W. A. *Bioorg. Med. Chem. Lett.* **2005**, *15*, 1457–1461.
(64) Sugishima, M.; Higashimoto, Y.; Oishi, T.; Takahashi, H.; Sakamoto, H.; Noguchi, M.; Fukuyama, K. *Biochemistry* **2007**, *46*, 1860–1867.

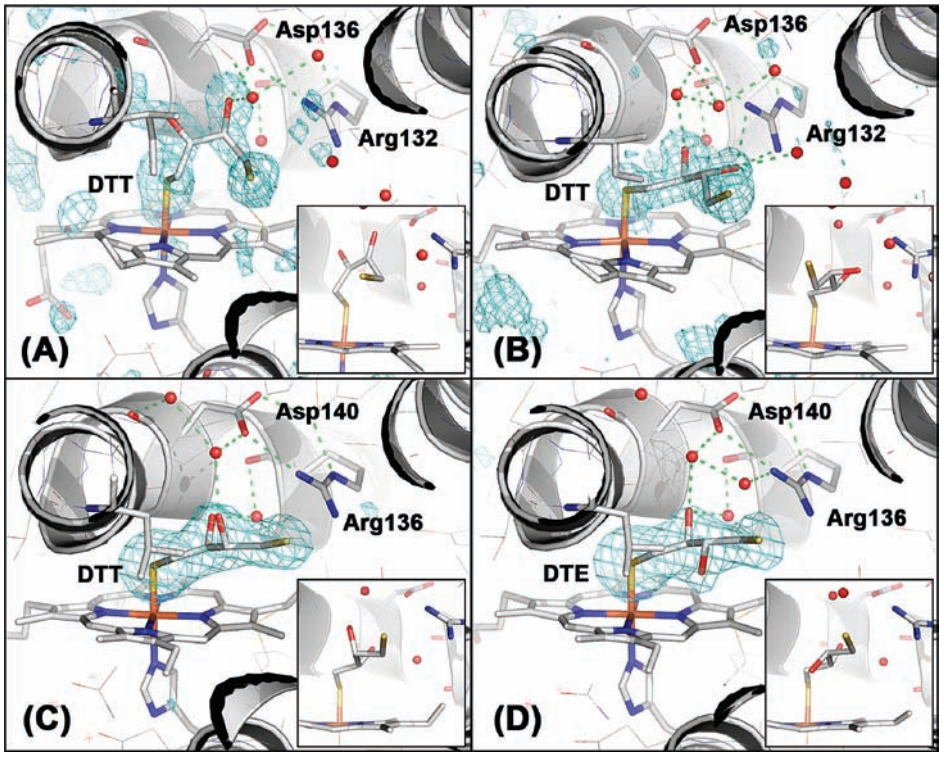

Figure 8. Active-site structures of the thiol-bound forms of ferric heme−HO complexes. (A and B) Molecules A and B of the DTT−heme−HmuO complex and (C and D) DTT- and DTE-bound forms of heme−rat HO-1 complexes, respectively. The omit F_o-F_c maps (cyan) contoured at 2.7σ and 3.5σ levels, respectively, for HmuO and HO-1 were calculated with their final models lacking the thiolate ligands. Insets: Alternative views from different angles.

group of DTT should be critical for its high affinity to the mammalian HO. In contrast, HmuO exhibits similar affinity for DTT, DTE, and thioglycerol (Table 1), indicating no functionality of the noncoordinating thiol group in complex formation with this bacterial HO.

The crystal structure of the DTT-bound form of the ferric heme−HmuO complex has been solved at 1.50 Å resolution (Figure 8, panels A and B, and Table 2). The asymmetric unit of the HmuO crystal contains three molecules, termed molecules A−C. Conformations of DTT in molecules B and C are similar to each other (Figure 8B), whereas that in molecule A is distinct from the others (Figure 8A). In all three HmuO molecules, DTT binds to the heme iron at one terminal thiol group, and two hydroxy groups interact with environmental amino acids (Arg132 and Asp136) and water molecules as designed (Figure 7). The noncoordinating thiol group locates in a hydrophobic pocket and does not appear to form a strong interaction, consistent with its minimal effect on the affinity to HmuO (Table 1).

Crystal structural analysis of mammalian HO was successful only for rat HO-1 in its DTT- and DTE-bound forms (Figure 8, panels C and D, and Table 2). The heme−rat HO-1 complex shows similar binding affinities of the DTT derivatives to those of the human counterpart (Table 1). In the DTT−heme−rat HO-1 complex (Figure 8C), the noncoordinating thiol group locates at a position close to the distal Arg (Arg136) residue [$d(S_{thiol}-N_{Arg})$ = 3.5 and 3.7 Å], suggesting an ionic interaction between the cationic guanidium and the thiolate anion to stabilize the heme-bound thiol. The DTE molecule also places its terminal thiol group at a similar position (Figure 8D); however, the thiol group appears to be moving away from the Arg residue [d(S−N) = 3.8 and 4.1 Å]. The noncoordinating thiol groups do not appear to stabilize the heme-bound DTT and DTE because their dissociation rate constants from the heme iron are very similar to that of thioglycerol in rat HO-1 (1.21, 0.96, and 0.94 s^{-1} for DTT, DTE, and thioglycerol, respectively).[72] The high affinity of DTT and DTE is mainly attributable to their 20−40-fold faster *association* than thioglycerol (256, 141, and 6.3 mM^{-1} s^{-1} for DTT, DTE, and thioglycerol, respectively).[72] Although the acceleration mechanism of the thiol association has yet to be clarified, the thiol−Arg interaction appears to help the incorporation of DTT and DTE into the distal pocket at a preequilibrium stage.

Thiol binding significantly suppresses but does not completely interrupt the reduction of the ferric heme to the

(65) Sugishima, M.; Sakamoto, H.; Higashimoto, Y.; Omata, Y.; Hayashi, S.; Noguchi, M.; Fukuyama, K. *J. Biol. Chem.* **2002**, *277*, 45086–45090.
(66) Otwinowski, Z.; Minor, W. *Methods Enzymol.* **1997**, *276*, 307–326.
(67) Brunger, A. T.; Adams, P. D.; Clore, G. M.; DeLano, W. L.; Gros, P.; Grosse-Kunstleve, R. W.; Jiang, J. S.; Kuszewski, J.; Nilges, M.; Pannu, N. S.; Read, R. J.; Rice, L. M.; Simonson, T.; Warren, G. L. *Acta Crystallogr., Sect. D: Biol. Crystallogr.* **1998**, *54*, 905−921.
(68) Schomaker, V.; Trueblood, K. *Acta Crystallogr., Sect. B: Struct. Crystallogr. Cryst. Chem.* **1968**, *24*, 63–76.
(69) CCP4: Collaborative Computational Project, **1994**, Number 4, Vol. *50*.
(70) Kleywegt, G. J.; Jones, T. A. *Acta Crystallogr., Sect. D: Biol. Crystallogr.* **1998**, *54*, 1119–1131.
(71) DeLano, W. L. *The PyMOL Molecular Graphics System*; DeLano Scientific LLC: Palo Alto, CA, **2002**.
(72) Kinetic analysis of the thiol binding at 20 °C in 0.1 M potassium phosphate buffer, pH 7.0, was performed by using a UNISOKU RSP-601 stopped-flow apparatus equipped with a built-in rapid-scan spectrophotometer. Observed binding rates of the thiols showed a good linear relationship with their concentrations to afford association rate constants. Dissociation rate constants of the thiols were calculated from their association rates and equilibrium dissociation constants (Table 1).

Table 2. Statistics of Data Collection and Structure Refinement for the Thiol-Bound Forms of Ferric Heme−HO Complexes[a]

	DTT−HmuO	DTT−rat HO-1	DTE−rat HO-1
PDB code	3I8R	3I9T	3I9U
beamline	Photon Factory AR NW12	SPring-8 BL38B1	Photon Factory BL-6A
	Crystal Data		
space group	$P2_1$	$P3_221$	$P3_221$
cell parameters			
a (Å)	54.12	65.75	65.88
b (Å)	62.56	65.75	65.88
c (Å)	108.00	120.67	120.24
β for HmuO, γ for rat HO-1 (deg)	100.67	120	120
	Data Collection		
molecules in an asymmetric unit	3	1	1
resolution range (Å)	50.0−1.50 (1.55−1.50)	50.0−2.15 (2.17−2.15)	50.0−2.25 (2.33−2.25)
total no. of observed reflns	773 048	108 593	107 098
total no. of unique reflns	111 073	17 047	14 964
I/σ	45.4 (2.62)	35.1 (4.05)	32.1 (7.04)
completeness (%)	98.0 (90.1)	100.0 (100.0)	99.9 (99.9)
R_{sym}	0.050	0.083	0.062
	Structure Refinement		
resolution range (Å)	20.0−1.50	50.0−2.15	30.0−2.25
no. of non-hydrogen protein atoms	4961	1729	1711
no. of water molecules	484	135	101
R	0.194	0.162	0.167
R_{free}	0.224	0.209	0.223
rms deviations from ideal geometry			
bond length (Å)	0.030	0.025	0.024
bond angle (deg)	2.519	1.916	1.913

[a] Crystals of thiol-bound forms were prepared by soaking single crystals of the ferric heme complexes of HmuO[34] and rat HO-1[65] with crystallization solutions containing DTT or DTE (100 and 5 mM for HmuO and rat HO-1, respectively). Intensity data collected at 100 K were integrated, merged, and processed with HKL2000.[66] Structures were determined by molecular replacement and rigid-body refinement by CNS.[67] The starting models used were the azide-bound form of the heme−rat HO-1 complex (PDB code: 1IVJ) for DTT−rat HO-1 and DTE−rat HO-1 and the ferric heme complex of HmuO (PDB code: 1IW0) for DTT-HmuO. The models were further refined using the maximum-likelihood target and TLS refinement[68] with REFMAC5.[69] The first starting model, topology, and parameter files of DTT were obtained from the HIC-Up server (http://alpha2.bmc.uu.se/hicup/).[70] DTE starting model, topology, and parameter files were produced from the corresponding files of DTT. Throughout the model building and refinement process, 10% of the reflections were excluded to monitor the R_{free} value. The drawings were made by PyMol.[71]

ferrous state. HO is inhibited thus at higher thiol concentration than expected from the dissociation equilibrium constants (Table 1); e.g., IC_{50} values of DTE are 17 and 1200 μM for human HO-1 and HO-2, respectively. For stronger inhibition, the inhibitor should be a ligand to ferrous heme iron and/or ferrous verdoheme iron to block O_2 binding. Although DTT and DTE are not practical inhibitors of HO per se, the 70-fold difference in the IC_{50} values indicates that the distal hydrogen-bonding network is a promising target for the future development of HO isoform selective inhibitors.

Concluding Remarks

The HO reactions are unique in that the substrate heme and its catabolic intermediates activate molecular oxygen for their self-oxidation. In the first *meso*-hydroxylation, the FeOOH species is characterized as a key intermediate. It transfers its terminal OH group into the porphyrin ring with help from the active-site water molecule consisting of the distal hydrogen-bonding network. Further investigation on the first step is expected to establish a catalytic mechanism that reconciles experimental results with theoretical proposals. Our results indicate that the HO third step proceeds through OH transfer by FeOOH in a manner similar to that in the first step. Characterization of the reaction intermediates with O_2 and H_2O_2 and determination of the O_2 binding site will further untangle the ring-opening mechanism. We also have identified the catalytically critical distal structure as a potential target for HO specific inhibitors. The structure-based design in combination with a compound library search is expected to develop a practical isoform-selective HO inhibitor.

Acknowledgment. This work has been supported by Grants-in-Aid for Scientific Research (to M.I.-S., Grants 12147201, 17GS0419, 18370052, and 21350087, to T.M., Grants 18770103 and 20750125, and to M.U., Grants 18770080 and 20770076) from JSPS and MEXT, Japan. X-ray diffraction experiments at Photon Factory were conducted under the approved codes of 2003G118 and 2005G255.